

Incipient motion for gravel particles in clay-silt-gravel cohesive mixtures

Zulfequar Ahmad¹ · Umesh K. Singh¹ · Ashish Kumar²

Received: 5 December 2016 / Accepted: 4 November 2017 / Published online: 23 November 2017
© Springer-Verlag GmbH Germany, part of Springer Nature 2017

Abstract

Purpose Incipient motion plays an instrumental role in understanding various aspects of sediment transport, such as river bed aggradation and degradation, channel design, bank erosion, scour around bridge piers, and water quality issues.

Materials and methods Experiments were conducted to study the incipient motion of gravel particles in three types of bed material, i.e., gravels only, silt-gravel mixture, and clay-silt-gravel mixture. The clay content varied from 10 to 50% in the clay-silt-gravel mixture while silt and gravel were in equal proportion by weight. Samples were taken out from the prepared cohesive bed for the determination of their bulk density, unconfined compressive strength, and water content. The incipient motion was observed visually, which corresponded to the beginning of movement of gravel particles in the mixture. The shear stress corresponding to incipient motion was computed using measured flow depth and slope of water surface. The physical appearance of the top layer of cohesive bed was observed visually at the end of experiment.

Results and discussion The effects of clay content, water content, unconfined compressive strength, and bulk density of the mixture on the critical shear stress were investigated using the data collected in this study on clay-silt-gravel mixture along with the data from previous studies. A relationship is proposed

for the computation of critical shear stress of gravel particles in the cohesive mixtures. The physical appearance of the top surface of the bed for clay-silt-gravel mixture has also been investigated with varying percentages of clay content in the mixture.

Conclusions High clay percentage significantly increased the critical shear stress. The presence of silt lowers the critical shear stress especially when there is low clay content (up to 20%) in the mixture. The clay content along with the bulk density was found to be the dominant parameters that affect the incipient motion of the gravel particles in the cohesive mixtures. The proposed relationship for critical shear stress was found to be in good agreement with the observed ones.

Keywords Bulk density · Clay-silt-gravel · Critical shear stress · Incipient motion · Scour

1 Introduction

Incipient motion refers to a flow condition at which sediment present in the channel bed begins to move. The study of incipient motion plays an instrumental role in understanding the various aspects of sediment transport, such as river bed aggradation and degradation, stable channel design, stream bank erosion, scour around bridge piers, water quality issues, and effects of fine sediment on aquatic life. Studies on incipient motion are widely categorized in two parts, i.e., one for cohesionless sediment and another for cohesive sediment. The criteria for incipient motion of uniform cohesionless sediment have been well established and studied by several authors (Shields 1936; Iwagaki 1956; Yang 1973; Yalin and Karahan 1979). Shields curve (1936) has been widely used for the computation of critical shear stress of uniform cohesionless sediment. Brownlie (1981) presented a revised

Responsible editor: Rui Miguel Lage Ferreira

✉ Zulfequar Ahmad
zulffce@iitr.ac.in

¹ Department of Civil Engineering, Indian Institute of Technology Roorkee, Roorkee 247667, India

² Department of Civil Engineering, JUIT Waknaghat, Solan, Himachal Pradesh 173234, India

Shields curve and proposed an expression for the computation of dimensionless critical shear stress that can be expressed as

$$\tau_{*cc} = 0.22Y + 0.06(10)^{-7.7Y} \tag{1}$$

where

$$Y = \left(\sqrt{(\rho_s - \rho)gd^3 / \rho\nu^2} \right)^{-0.6} \tag{2}$$

Here, τ_{*cc} is the dimensionless critical shear stress for the cohesionless sediment; ρ_s and ρ are the particle and fluid densities (kg m^{-3}), respectively; g is the gravitational acceleration (m s^{-2}); d is the arithmetic mean size of the cohesionless sediment (m); and ν is kinematic viscosity ($\text{m}^2 \text{s}^{-1}$).

Yalin (1977) favors the method of visual observation for identification of incipient motion as he stated that “In practice one has no alternative but to identify the beginning of sediment transport with the sediment transport itself.” He presented the following mathematical expression for incipient motion for uniform cohesionless sediment:

$$\varepsilon = \frac{m}{\Omega T} \sqrt{\left(\frac{\rho d_{50,g}^5}{\rho_s g} \right)} \tag{3}$$

where m is the number of particle detachment observed, T is the time duration of observation, Ω is the surface area of mobile bed, and $d_{50,g}$ is the d_{50} of gravel particle. For incipient condition, $\varepsilon > 0$ and should have a constant value. In the present study, m is taken as the mass (in newtons) of detached particles in place of the number of particles detached for the computation of ε .

Various studies have investigated non-uniform cohesionless sediments (Parker et al. 1982; Bridge and Bennett 1992; Patel and RangaRaju 1999; Wu et al. 2000; Aberle and Nikora 2006; Gaucher et al. 2010). Incipient motion of the non-uniform sediment is complex compared to that of the uniform cohesionless sediment as the movement of particles in a non-uniform sediment mixture is characterized by their unequal mobility especially when the mixture comprises of fine to coarse sediment like silt-gravel. The unequal mobility of particles has been analyzed as the fraction-wise movement of particles present in the sediment mixture (Kuhnle 1993; Patel and RangaRaju 1996; Dong 2007).

River bed is often consists of a mixture of cohesive as well as cohesionless materials. Singh et al. (2007) reported that the Ganga river bed is consisted of sediment having clay, silt, sand, and gravel. Jain (2008) reported the presence of clay, sand, and gravel mixture on the bank of the river Ganga at Rishikesh, India. The erosion characteristic of cohesive sediment is significantly different from cohesionless sediment due to dominancy of physio-chemical properties of the cohesive sediment (Kothyari and Jain 2010). On mixing the cohesionless sediment with cohesive sediment, the resulting mixture

possesses a certain amount of cohesive property (Mitchener and Torfs 1996; Kothyari and Jain 2010); therefore, that is treated as a cohesive sediment mixture.

In the past, several experimental studies have been conducted on incipient motion for different cohesive sediment mixtures like clay-sand, clay-silt-sand, clay-gravel, and clay-sand-gravel (Kamphuis and Hall 1983; Mitchener and Torfs 1996; Ansari et al. 2007; Kothyari and Jain 2008; Ahmad et al. 2011; Ikari and Kopf 2011). Based on the experimental study on cohesive mixture of clay-silt-sand, Kamphuis and Hall (1983) concluded that the critical shear stress increases linearly with unconfined compressive strength. They reported higher resistance of channel bed against erosion for higher clay content and plasticity index. Mitchener and Torfs (1996) reported that the bulk density of mud-sand cohesive mixture increases with an increase in clay content. Kothyari and Jain (2008) conducted the experimental study on incipient motion for a cohesive mixture of clay-gravel and clay-sand-gravel in which clay content was varied from 10 to 50%. They concluded that the critical shear stress increases with an increase of clay content and unconfined compressive strength while decreases with an increase of void ratio. Dong (2007) pointed out that the incipient motion for gravel-silt mixture has different behaviors than that for gravel-sand mixture when compared with the Shields curve. The presence of silt in the mixture may result in significant changes in critical shear stress when compared with a silt-free mixture. Kothyari and Jain (2008) reported the incipient motion for the cohesive sediment mixture of clay-gravel. The presence of silt with gravel particles in cohesive mixture has not been studied so far. The present study focuses on the incipient motion for gravel particles in the mixture of clay-silt-gravel. An attempt has been made to develop a relation to compute the critical shear stress of gravel particles in cohesive sediment mixture.

To investigate the effect of clay percentage present in the mixture, the critical shear stress has been compared with the cohesionless sediment having same mean size as that of cohesive sediment mixture. Dimensionless critical shear stress and unconfined compressive strength for cohesive sediment mixture has been computed as

$$\tau_{*cc} = \tau_{cc} / (\rho_s - \rho)gd_a \tag{4}$$

$$UCS^* = UCS / (\rho_s - \rho)gd_a \tag{5}$$

$$d_a = \sum(d_{50}P) / \sum P \tag{6}$$

Here, τ_{*cc} is the dimensionless critical shear stress of cohesive sediment mixture, τ_{cc} is the critical shear stress of cohesive sediment mixture (N m^{-2}), UCS is the unconfined compressive strength of cohesive sediment mixture (N m^{-2}), UCS* is the dimensionless UCS, d_a is the arithmetic mean size of the cohesive sediment mixture (m), d_{50} is the sediment size (m)

such that 50% of material is finer than that size by dry weight, and P is the percentage of the individual sediment in the sediment mixture.

The sensitivity analysis has been carried out using statistical parameters of correlation coefficient (r), root mean square error (RMSE), mean absolute percentage of error (MAPE), BIAS, and scatter index (SI) as per following equations (Najafzadeh and Lim 2015):

$$r = \frac{\sum_{i=1}^N (Y_{i(Actual)} - \bar{Y}_{(Actual)}) (Y_{i(Model)} - \bar{Y}_{(Model)})}{\sqrt{\sum_{i=1}^N (Y_{i(Actual)} - \bar{Y}_{(Actual)})^2 \sum_{i=1}^N (Y_{i(Model)} - \bar{Y}_{(Model)})^2}} \quad (7)$$

$$RMSE = \left[\frac{\sum_{i=1}^N (Y_{i(Model)} - Y_{i(Actual)})^2}{N} \right]^{1/2} \quad (8)$$

$$MAPE = \frac{1}{N} \left[\frac{\sum_{i=1}^N |Y_{i(Model)} - Y_{i(Actual)}|}{\sum_{i=1}^N Y_{i(Actual)}} \times 100 \right] \quad (9)$$

$$BIAS = \frac{\sum_{i=1}^N (Y_{i(Model)} - Y_{i(Actual)})}{N} \quad (10)$$

$$SI = \frac{RMSE}{(1/N) \sum_{i=1}^N Y_{i(Actual)}} \quad (11)$$

2 Experimental set-up and observations

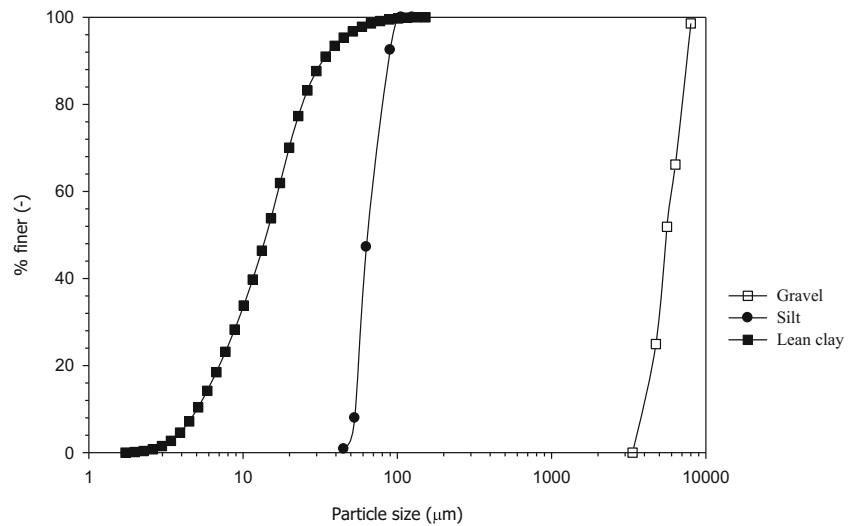
Experiments were conducted on a tilting flume having 16 m length, 0.75 m width, and 0.50 m depth in the Hydraulic Engineering Laboratory, Civil Engineering Department, Indian Institute of Technology Roorkee, Roorkee, India. The channel had a test section of 6.0 m length, 0.75 m width, and 0.18 m depth and located at a distance of 7.0 m from the channel entrance. The median size (d_{50}) of clay, silt, and gravel in the mixture was 0.014, 0.062, and 5.50 mm, respectively, as illustrated in Fig. 1, and the geometric standard deviations were 2.06, 1.18, and 1.31, respectively. Clay used in the present study is classified as lean clay according to the Unified Soil Classification System (ASTM D2487 2011). The geometric standard deviation was computed as $0.5[(d_{84}/d_{50}) + (d_{50}/d_{16})]$ (Garde and RangaRaju 2000), where d_{84} , d_{50} , and d_{16} are the sediment size such that 84, 50, and 16% of material are finer than those of the size by weight, respectively. Various properties of the clay used in the present study are given in Table 1.

The incoming flow in the flume was regulated with the help of a valve fitted in the supply. The discharge measurement was done volumetrically using a tank provided at the end of the flume. A rectangular trap, which was placed at the end of the flume just after the tail gate, was used for the collection of the bed load. A two-dimensional bed-level profiler having a resolution of 1.0 mm was used to measure the profile of the channel bed. The water surface profile was measured with the help of a point gauge having the least count of 0.10 mm. Bed and water surface profile measurements were taken at a longitudinal spacing of 0.50 m along the center line of the flume.

In the mixtures of clay-silt-gravel, the percentage of clay was varied from 10 to 50% on weight basis while the other sediments (i.e., silt and gravel) were taken in equal proportions. Channel bed in the test section was prepared by taking dry weight of sediment as per proportions and then manually mixed together with water. After mixing, the sediment was covered with polythene and left for 24 h for uniform moisture distribution and finally filled in the test section and compacted in three equal layers. Each layer was compacted by passing a cylindrical roller over it having a weight equal to 400 N while the sides of channel were compacted by a hand rammer having rectangular bottom. Bed preparation has been done under control condition by allowing the equal number of passes (ten passes, i.e., five rounds) of cylindrical roller over the test section in each layer. Extra sediments were chiseled off using a sharp-edge large knife after compacting all the three layers, and finally, the prepared cohesive bed was left for about 16 h in order to achieve the cohesive bonding between the cohesive and non-cohesive matrices. Figure 2a shows the preparation of cohesive mixture while Fig. 2b shows the prepared cohesive bed. Samples were taken out from the downstream section of prepared cohesive bed for the determination of bulk density, unconfined compressive strength, and water content. After taking the sample, the hole was filled and hammered in order to maintain the prepared cohesive bed. Before the beginning of the experimental run, bed was saturated for 24 h in order to achieve the field's condition (Jain 2008). For all the experimental runs, the sediment beds were prepared afresh. The water content of the sample was computed as per an oven-dry method. The bulk density was computed as per a standard core cutter method (IS 1975). Void ratio has been computed with the help of bulk density. The unconfined compressive strength of the sample was measured in the laboratory with the help of unconfined compression test apparatus as shown in Fig. 3.

The incipient motion condition of gravel particles was determined in a clay-silt-gravel mixture bed, gravel bed, and silt-gravel mixture bed. Initially, the experiment was conducted for gravel bed only, then silt was mixed with gravel particles in equal proportion and incipient motion was investigated for gravel particles. After that, the experiment on incipient motion

Fig. 1 Size distribution of sediments



of gravel particles was conducted for the cohesive mixture of clay-silt-gravel in which clay content was varied from 10 to 50% by weight.

3 Incipient motion

After channel bed preparation, initially low discharge was allowed in the flume and uniform flow was maintained by operating the tail gate. Then, a small increment in the discharge was allowed and the sediment bed was observed visually during the process in order to examine the detachment of the gravel particles. The flow condition, at which the detachment of gravel particles begins, was treated as the incipient motion condition. At this flow condition, measurement of discharge, water surface profile, and bed surface profile were taken. Visual observation method to identify incipient motion condition has been adopted earlier by Kothyari and Jain (2008). The mean velocity of flow was computed using measured discharge and flow depth. Flow depth was computed as

an average of differences between the measured bed and water surface profiles at the middle of each section. The shear stress, corresponding to incipient motion, was computed using the measured flow depth and slope of water surface.

Appearance of the top surface of the bed was analyzed visually after the end of incipient motion for each run. It was noticed that the appearance of the top surface of bed varied with the percentage of the clay in the sediment mixture of clay-silt-gravel. For low clay content (i.e., up to 20%), the fine particles (i.e., silt and clay) went into suspension and washed away along with the flow, leaving the coarser (i.e., gravel) particles on the top surface of the bed. This may be attributed to high silt content and low clay content in the sediment mixture which might not be able to bind the sediment particles together and resulted in rapid suspension of fine (clay and silt) particles. The appearance of gravel particles on the top surface of the bed was less dominating as clay percentage increases from 10 to 50% as illustrated in Fig. 4. An increase in clay percentage from 20 to 30% in the mixture resulted in a stronger bond among the particles. Patterns of line and mass

Table 1 Clay properties

Clay properties	Value	Method used
Liquid limit	38.90%	Casagrande apparatus
Plastic limit	19.90%	By making threads of 3.00 mm dia.
Plasticity index	19.00%	= (Liquid limit – Plastic limit)
Maximum dry density	1.70 g cm ⁻¹	Standard proctor compaction test
Optimum moisture content	18.00%	
Cohesion	28.59 kN m ⁻²	Triaxial shear test
Angle of internal friction	31.8°	
Relative density	2.60	Pycnometer test
Clay mineralogy	Kaolinite 78% Illite 17% Montmorillonite 5%	X-ray diffraction test



Fig. 2 a Mixture preparation and b prepared channel bed for clay-silt-gravel mixture

erosions were noticed in few runs with 20 and 30% clay content, respectively, in the mixture of clay-silt-gravel. However, it was observed that line erosion was dominant in case of 30% clay content and mass erosion in case of 40–50% clay content in the mixture. For the clay percentage of 40 and 50%, it was observed that particles were eroded in the form of bunch or chunks as the bonding between the particles was much stronger due to the cohesive nature of the clay particles. Mass erosion was prominent upstream of the test section. The



Fig. 3 Sample before and after the test in the unconfined compression test apparatus

physical appearances of the top surface of the eroded bed for different clay contents are shown in Fig. 4a–d for illustration.

A visual observation method to identify the incipient motion condition has been adopted in the present study as per Kothyari and Jain (2008) along with Yalin (1977) criteria of incipient motion. As per Yalin (1977) criteria, parameter (ε) (in Eq. (3)) should have a constant value for each experimental run and, to achieve this, the three parameters (i.e., $(\Omega/d_{50,g}^2)$, $(T\sqrt{\rho_s g/\rho d_{50,g}})$, and (m)) should be constant for each experimental run. The first two parameters have constant values of 148,760.3 and 82,500.6, respectively, for all experiments in the present study, and the third parameter (i.e., the mass parameter (m)) varied in a close interval of 0.9 to 1.98. Hence, the Yalin parameter (ε) has nearly the constant value in a close interval of 7.35×10^{-11} to 16.15×10^{-11} which indicates that the present study follows the Yalin criteria for incipient motion.

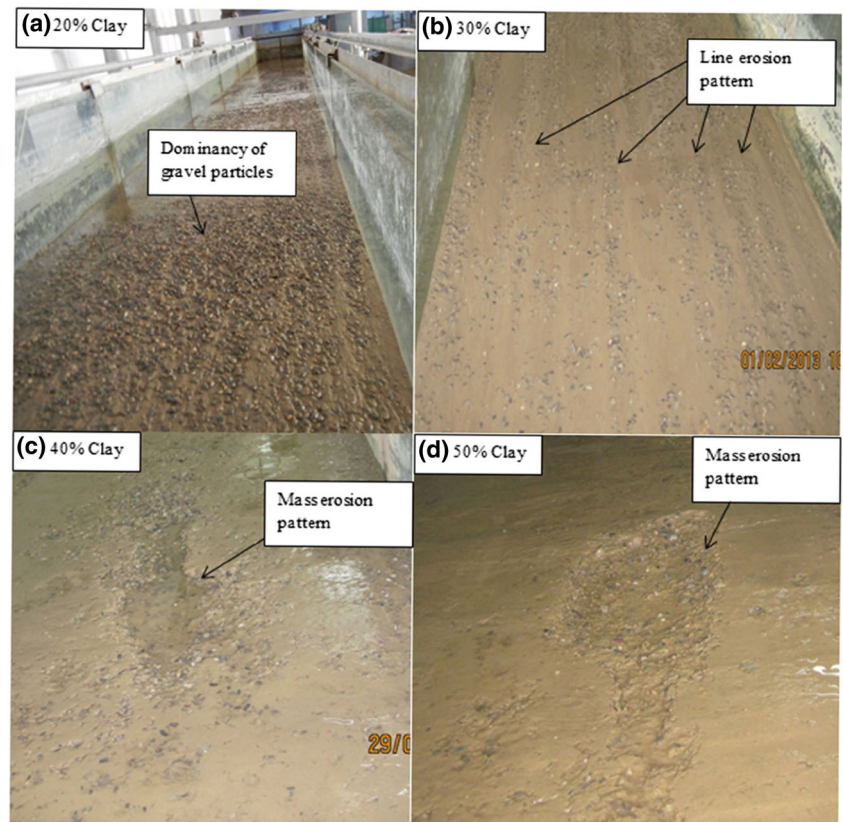
4 Results and discussion

4.1 Parameters affecting incipient motion

The probable parameters that influence critical shear stress of particles in the cohesive sediment mixture are clay content (P_c), ratio of water content to optimum water content (W/W_p), dimensionless unconfined compressive strength (UCS*), and dimensionless bulk density (ρ_b/ρ). Variations of these parameters with τ_{*cc} are shown in Figs. 5, 6, 7, and 8, respectively. The data of the present study on clay-silt-gravel mixture along with the data of Kothyari and Jain (2008) on clay-gravel mixture have been used in this study. The range of parameters is given in Table 2.

Figure 5 shows that the value of τ_{*cc} increases with the increase of clay content from 10 to 50% for the mixtures of clay-gravel and clay-silt-gravel. An increase of clay percentage in the sediment mixture makes the stronger bond among the sediments present in the mixture due to its dominating physio-chemical properties and resulted in high erosion resistance against the flow that leads to a higher value of critical shear stress. Dimensionless critical shear stress is noticed to be higher in magnitude for clay-gravel mixture when compared with clay-silt-gravel mixture for 10–30% of clay content in their mixture. However, for higher clay content (i.e., 40–50%), the dimensionless critical shear stress for clay-silt-gravel mixture is higher than that of clay-gravel mixture, which may be attributed to the weight of larger size of gravel (5.5 mm) in clay-silt-gravel mixture than that of gravel size (3.1 mm) in clay-gravel mixture. However, a low value of τ_{*cc} for clay-silt-gravel mixture than that of clay-gravel mixture (for 10–30% clay) may be attributed to high silt content in the clay-silt-gravel mixture.

Fig. 4 a–d Physical appearance of the top surface of bed after the incipient motion runs for clay-silt-gravel mixture



The water content of sediment mixtures in respect to the ratio of water content (W) to optimum water content (W_p) plays a significant role in the detachment of soil particles from the channel bed. For low water content (i.e., $[(W/W_p) < 1]$), attractive forces are dominant among the soil particles that result in the detachment of soil particles in flocculated structures, however; in case of high water content (i.e., $[(W/W_p) > 1]$), repulsive forces increase that leads to orientation of

particle into dispersed structure (Shroff and Shah 2003). Figure 6 shows a plot between τ_{*cc} and W/W_p for the clay-silt-gravel mixture for varying clay contents of 10 to 50% which indicates high critical shear stress for high clay content mixture having W/W_p close to unity or less. It is also clear that W/W_p is less than unity for most of the data points having high clay content (40–50%) in the sediment mixture and greater than unity for low clay content (10–20%) in the mixture.

Fig. 5 Variation of τ_{*cc} with clay percentage in fraction

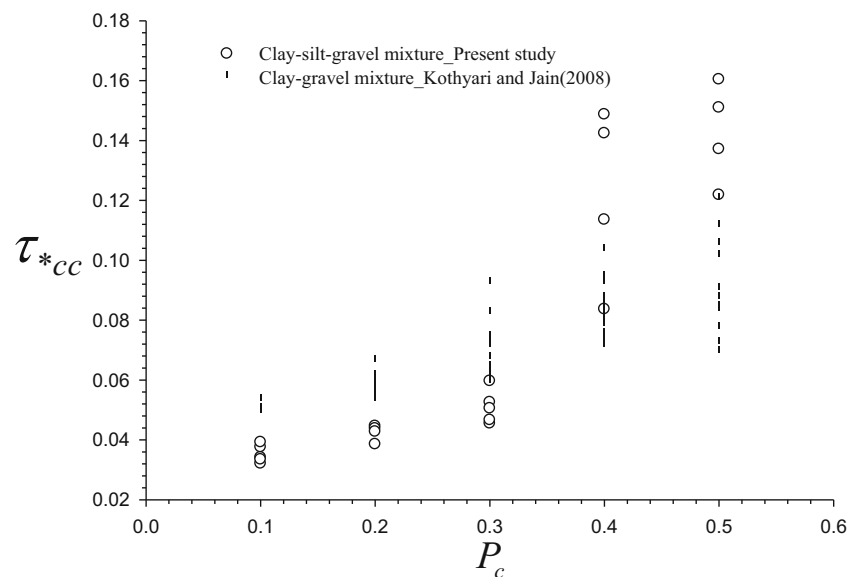
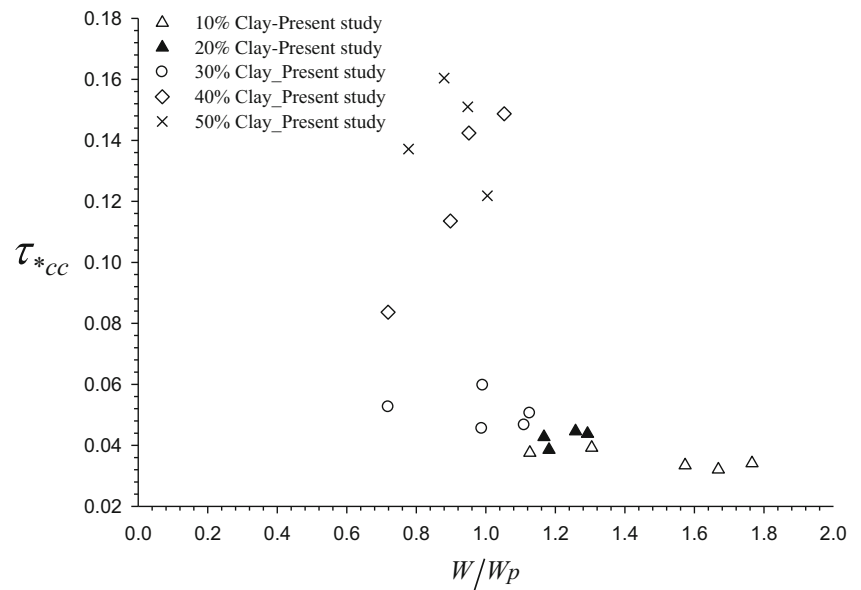


Fig. 6 Variation of τ_{*cc}^{*cc} with water content in fraction



This may be caused to flocculate and dispersion structure of soil for high and low clay content in the mixture, respectively. Figure 6 depicts low and high critical shear stress for the same range of W/W_p at 0.8–1.0 which attributed to the variation of clay content in the mixture. High clay content in the mixture provides higher strength to bed, and it leads to higher critical shear stress.

UCS test has been conducted for the compactness of cohesive bed. A plot between τ_{*cc} and UCS* is shown in Fig. 7 which depicts that τ_{*cc} increases with the increase of UCS* for both the mixtures, i.e., clay-silt-gravel and clay-gravel. It has been noticed that UCS increases with the increase of clay percentage. High clay content enhances compactness of the cohesive bed and becomes highly resistive against load failure which resulted in a higher value of UCS.

Figure 8 reveals that τ_{*cc} increases with an increase of bulk density. For the same clay percentage, bulk density for clay-gravel mixture is higher than that of clay-silt-gravel mixture

especially for the 10 to 30% of clay content in the mixture. It may be attributed to the presence of higher silt content. Noted that both UCS and water content affect the bulk density.

Void ratio is an alternate parameter for bulk density that affects the bonding among the particles in the sediment mixture. Figure 9 shows the data for void ratio for the clay-silt-gravel mixture of the present study along with the data for the clay-gravel mixture of Kothyari and Jain (2008) to illustrate the effect of the presence of silt in the cohesive mixture. A higher value of void ratio for clay-silt-gravel mixture than that of clay-gravel mixture as illustrated in Fig. 9 leads to a weaker bond among the particles for clay-silt-gravel mixture. The data on compressive strength of different sediment beds in terms of unconfined compressive strength are illustrated in Fig. 9 which indicate an increase of strength of bed with the increase of clay content in the mixture.

It may be concluded that clay content, water content, and compaction are the main factors that govern the incipient

Fig. 7 Variation of τ_{*cc}^{*cc} with UCS*

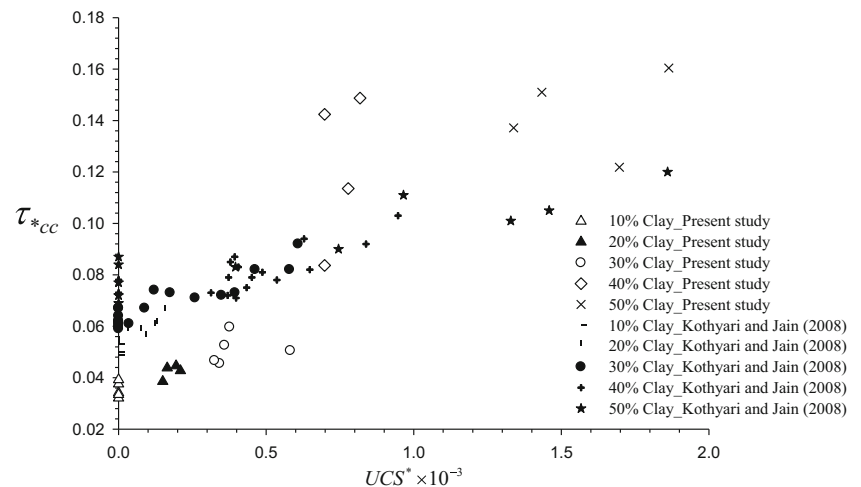
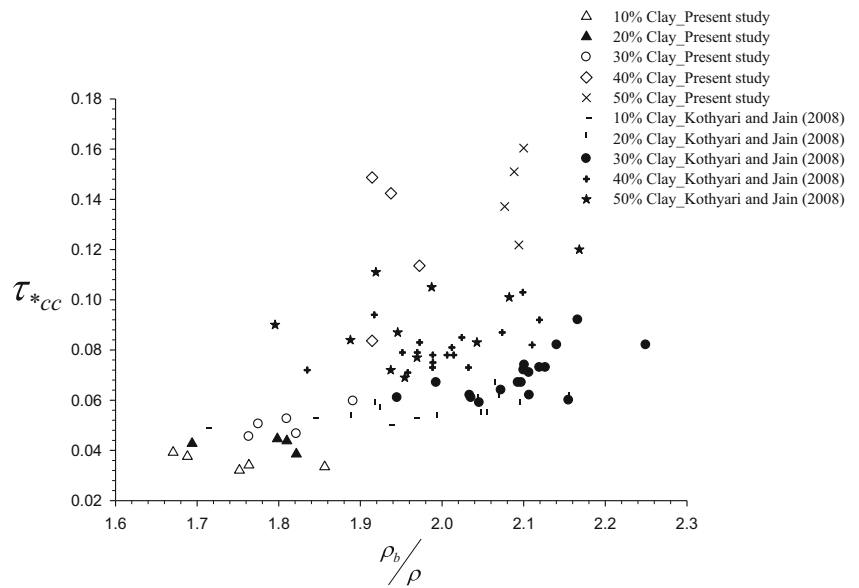


Fig. 8 Variation of τ_{*cc} with (ρ_b/ρ)



motion; however, the effect of clay content is more pronounced. As water content in the mixture and UCS govern the bulk density, it is appropriate to consider clay content and bulk density as governing parameters for the incipient motion of cohesive mixture in addition to the sediment size.

4.2 Effect of clay and silt contents on incipient motion

Effect of clay content and sediment size on incipient motion was analyzed by plotting the dimensionless critical shear stress (τ_{*cc}) and particle Reynolds number (R_*) on the revised Shields curve (Brownlie 1981) as shown in Fig. 10. Approximation of Shields curve as per Cao et al. (2006) has also been included in Fig. 10 which is close to Brownlie (1981) especially for high-particle Reynolds number.

Buffington and Montgomery (1997) reviewed the eight-decade data on incipient motion for gravel-bedded river and reported the range of dimensionless critical shear stress as 0.030–0.073 for visually based study of incipient motion of gravel particles. Rouse (1939) reported the dimensionless critical shear stress for gravel bed as 0.056 (Bunte et al. 2010). In the present experimental study, dimensionless critical shear stress in pure gravel was observed in the range of 0.05–

0.052 which is very close to the Shields value as per revised Shields curve (Brownlie 1981) as well as in good match with the other studies, i.e., Rouse (1939) and Buffington and Montgomery (1997).

The value of τ_{*cc} for gravel in clay-gravel mixture lies above the revised Shields curve while, for only gravel bed, τ_{*cc} lies close to the revised Shields curve. This may be due to the presence of clay which makes the cohesive bond between particles and causes more resistance of sediment movement against the flow.

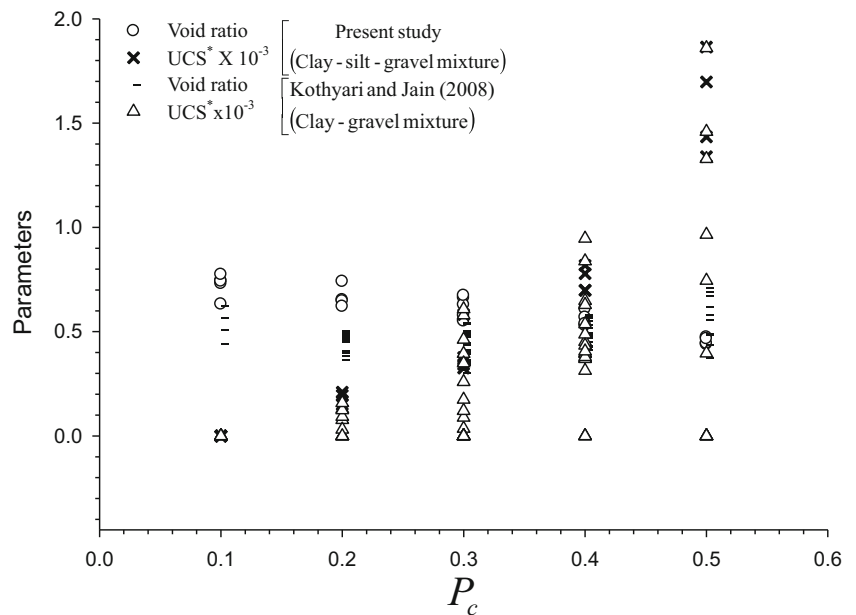
Investigation of incipient motion of gravel in gravel bed and silt-gravel bed indicates that the presence of silt in the gravel decreases the critical tractive shear stress as illustrated in Fig. 10. This is attributed to exposure of gravel particles due to dislodging of silt at low tractive shear stress.

The addition of clay with silt-gravel mixture has been analyzed for incipient motion of gravel particles by plotting the value of τ_{*cc} for clay-silt-gravel mixture on the revised Shields curve (Fig. 10). It can be noticed that the dimensionless critical shear stress for silt-gravel mixture lies below the revised Shields curve and even below the 10% of clay content in the mixture of clay-silt-gravel which may be attributed to higher silt content and no clay content in the mixture.

Table 2 Range of parameters for incipient motion

Study	Sediment mixture	Clay %	Arithmetic mean size (μm)	Mean flow depth (m)	Mean flow velocity (m s^{-1})	Water surface slope (-)	Dimensionless critical shear stress (-)
Present study	Gravel	0	5500	0.070–0.097	0.816–0.884	0.0051–0.0085	0.05–0.052
	Silt-gravel	0	2781	0.024–0.025	0.364–0.398	0.0077–0.0105	0.028–0.034
	Clay-silt-gravel	10–50	1397.5–2504.3	0.023–0.059	0.306–0.902	0.0045–0.0123	0.032–0.16
Kothyari and Jain (2008)	Clay-gravel	10–50	1552–2790.4	0.028–0.15	0.526–0.848	0.0023–0.0098	0.049–0.12

Fig. 9 Variation of void ratio and UCS* with clay fraction



The presence of silt has also been analyzed by comparing the value of τ_{*cc} for clay-silt-gravel mixture against the mixture of clay-gravel. It can be seen that all data of Kothyari and Jain (2008) lie above the revised Shields curve (Fig. 10) for clay-gravel mixture. However, the value of τ_{*cc} for clay-silt-gravel mixture lies above the revised Shields curve for clay content of 30 to 50% while the values of τ_{*cc} for 10 and 20% clay content lies below the revised Shields curve. This is because of not achieving the proper compaction level due to higher silt content and low clay content in the mixture which

leads to dislodging of fine particles along with the flow and resulted in exposure of gravel particles, and it causes lower critical shear stress. Due to the weak bond among the particles under the high silt and low clay content (for 10 and 20% clay content) in the clay-silt-gravel mixture, the fine particles (clay and silt) move early, followed by gravel particles. The early movement of the fine particles disturbs the position of gravel particles as the gravel particles are surrounded by the fine particles which leads to the movement of gravel particles at less shear stress compared to the revised Shields curve. It may be

Fig. 10 Variation of dimensionless critical shear stress with the particle Reynolds number

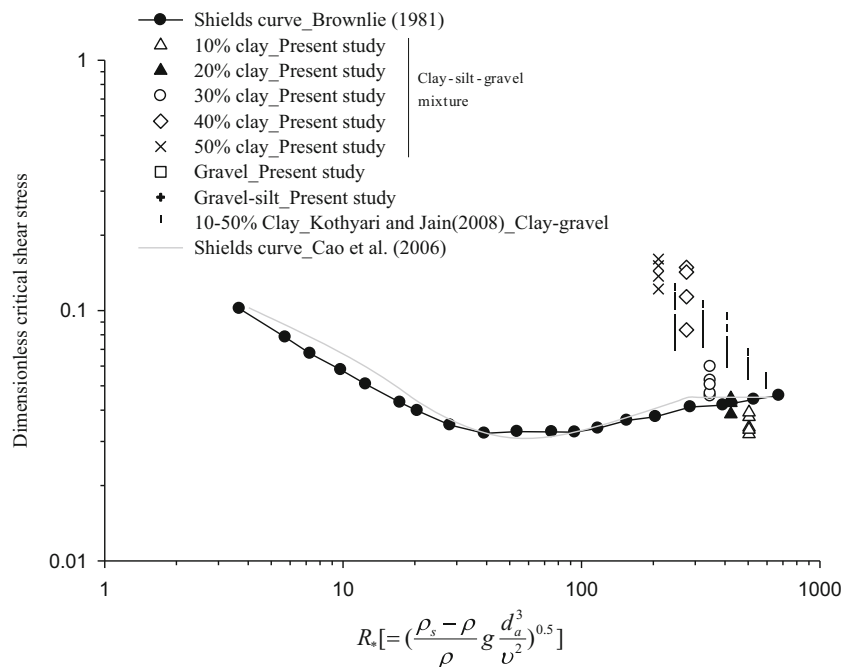
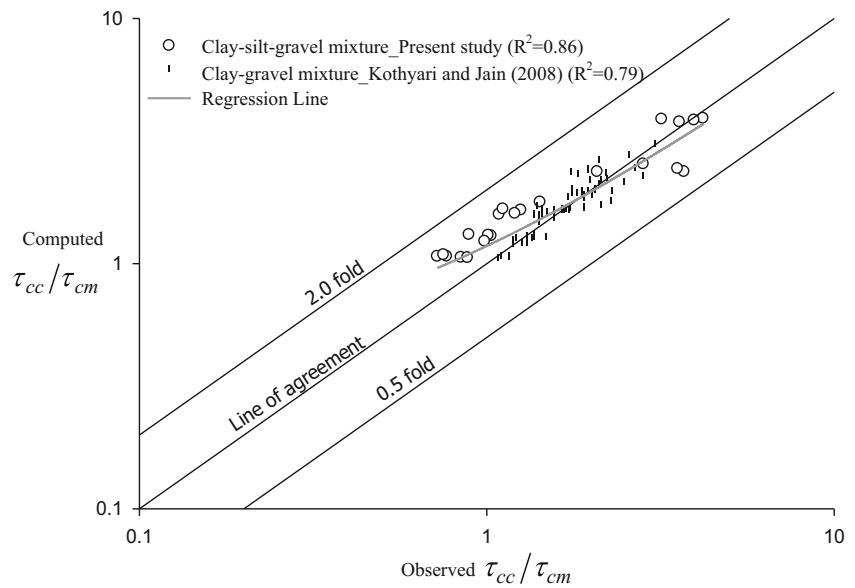


Fig. 11 Comparison of the observed and computed values of (τ_{cc}/τ_{cm}) using the proposed Eq. (15)



concluded that the presence of silt has a significant impact on the incipient motion of gravel particles present in sediment mixture especially when there is low clay content in the mixture.

4.3 Relationship for critical shear stress

A relationship has been developed for the computation of critical shear stress for the gravel particles present in the cohesive mixtures. The following variables are considered as a function of critical shear stress of gravel particles

$$\tau_{cc} = f(\tau_{cm}, P_c, P_s, \rho_b, \rho) \tag{12}$$

$$\tau_{cm} = \tau_{*cm}(\rho_s - \rho)gd_a \tag{13}$$

Here, τ_{cm} is the critical shear stress ($N\ m^{-2}$) for the cohesionless sediment, P_c is the clay content in fraction, P_s is the silt content in fraction, and ρ_b is the bulk density ($kg\ m^{-3}$) of the cohesive sediment mixture.

Equation (12) may be written in the dimensionless form as

$$\frac{\tau_{cc}}{\tau_{cm}} = f\left(P_c, P_s, \frac{\rho_b}{\rho}\right) \tag{14}$$

Equation (14) leads the following relationship for the computation of critical shear stress of gravel particles using the data of the present study of clay-silt-gravel mixture and Kothyari and Jain’s (2008) data of clay-gravel mixture:

$$\frac{\tau_{cc}}{\tau_{cm}} = 1 + 0.354P_c^{2.081}(1 + P_s)^{2.275}\left(\frac{\rho_b}{\rho}\right)^{4.10} \tag{15}$$

It may be noted that Eq. (15) converses to critical shear stress equation of Brownlie (1981) for cohesionless sediment in case of no clay content in the mixture.

The computed value of τ_{cc}/τ_{cm} from Eq. (15) has been plotted against the observed ones as shown in Fig. 11 which reveals that Eq. (15) predicts well the value of τ_{cc}/τ_{cm} as it is in good

Table 3 Results of sensitivity analysis

Functions	r	RMSE	MAPE	BIAS	SI
$\frac{\tau_{cc}}{\tau_{cm}} = f\left(P_c, P_s, \frac{\tau_{cc}}{\tau_{cm}}\right)$	0.91	0.31	0.49	0.06	0.04
$\frac{\tau_{cc}}{\tau_{cm}} = f\left(P_s, \frac{\tau_{cc}}{\tau_{cm}}\right)$	0.49	6.54	14.36	24.16	0.96
$\frac{\tau_{cc}}{\tau_{cm}} = f\left(P_c, \frac{\tau_{cc}}{\tau_{cm}}\right)$	0.85	0.43	0.56	-0.37	0.06
$\frac{\tau_{cc}}{\tau_{cm}} = f(P_c, P_s)$	0.84	1.02	1.74	-2.82	0.15

agreement with the observed ones. The proposed Eq. (15) has a good value of regression coefficient ($R^2 = 0.82$) for the data used in developing the equation. The data from Kothyari and Jain (2008) seem tighter around the line of agreement than that of author's data. However, the author's data are more supportive towards the regression line than that of Kothyari and Jain (2008) data as illustrated in Fig. 11 that leads to a higher regression coefficient for the author's data ($R^2 = 0.86$) than that of Kothyari and Jain (2008) data ($R^2 = 0.79$).

The sensitivity analysis has been performed for variables in the proposed Eq. (15) by using statistical parameters as per Eqs. (7)–(11). The sensitivity analysis is carried out by eliminating one variable each time from Eq. (15) to evaluate the impact of that input on the output. The result of sensitivity analysis in terms of statistical parameter is shown in Table 3. Table 3 indicates that the variable clay content (P_c) is the most sensitivity parameter while the other variables (ρ_b/ρ) and (P_s) have the least influence.

5 Conclusions

Results of an experimental study on incipient motion of gravel particles in the cohesive sediment mixture of clay-silt-gravel have been presented herein. The incipient motion of the gravel was visually observed, and the flow condition at which the gravel particles start to move is considered as incipient motion. The erosion pattern on the top surface of the bed was observed visually after the end of each run and found to vary with clay percentage. More gravel particles were noticed on the top surface of the bed for 10 and 20% clay content in clay-silt-gravel mixture. However, the dominance of gravel particles on the top surface was less for high clay percentage in the sediment mixture. A line erosion pattern was observed for 30% clay content while mass erosion pattern in the form of chunks was observed for 40 and 50% of clay content in the mixture. A high clay percentage in the mixture significantly increases the critical shear stress. The presence of silt has a significant impact on the incipient motion of gravel particles (as it lowers the critical shear stress) present in the sediment mixture, especially for low clay content (up to 20%). The clay content along with the bulk density was found to be the dominant parameters that affect the incipient motion of the gravel particles in the cohesive mixtures. The relationship proposed in the present study for the computation of critical shear stress of gravel particles is in good agreement with the observed ones.

Acknowledgements The experimental work presented here is the part of research project funded by the Indian Committee on Surface Water (INCSW), Ministry of Water Resources, Government of India.

References

- Aberle J, Nikora V (2006) Statistical properties of armored gravel bed surfaces. *Water Resour Res* 42:1–11
- Ahmad MF, Dong P, Mamat M, Nik WBW, Mohd MH (2011) The critical shear stresses for sand and mud mixture. *Appl Math Sci* 5: 53–71
- Ansari SA, Kothyari UC, RangaRaju KG (2007) Incipient motion characteristics of cohesive sediments. *ISH J Hydraul Eng* 13:108–121
- ASTM D2487 (2011) Standard practice for classification of soils for engineering purposes (unified soil classification system). ASTM International, West Conshohocken. <https://doi.org/10.1520/D2487-11>
- Bridge JS, Bennett SJ (1992) A model for the entrainment and transport of sediment grains of mixed sizes, shapes, and densities. *Water Resour Res* 28:337–363
- Brownlie WR (1981) Prediction of flow depth and sediment discharge. Report No. KH-R-43A, W. M. Keck Laboratory of Hydraulics and Water Resources, California Institute of Technology, Pasadena, California
- Buffington JM, Montgomery DR (1997) A systematic analysis of eight decades of incipient motion studies, with special reference to gravel-bedded rivers. *Water Resour Res* 33:1993–2029
- Bunte K, Abt SR, Swingle KW, Potyondy JP (2010) Bankfull mobile particle size and its prediction from a Shields-type approach. In: 2nd Joint Federal Interagency Conference, Las Vegas, NV
- Cao Z, Pender G, Meng J (2006) Explicit formulation of the Shields diagram for incipient motion of sediment. *J Hydraul Eng* 132: 1097–1099
- Dong P (2007) Two-fraction formulation of critical shear stresses for sand and silt mixtures. *J Waterw Port Coast Ocean Eng* 133:238–241
- Garde RJ, RangaRaju KG (2000) Mechanics of sediment transportation and alluvial stream problems, 3rd edn. New Age International, New Delhi
- Gaucher J, Marche C, Mahdi T-F (2010) Experimental investigation of the hydraulic erosion of noncohesive compacted soils. *J Hydraul Eng* 136:901–913
- Ikari MJ, Kopf AJ (2011) Cohesive strength of clay-rich sediment. *Geophys Res Lett* 38:1–5
- IS (Bureau of Indian Standards) (1975) Determination of in-place density by core-cutter method. IS-2720, Part XXIX, New Delhi
- Iwagaki Y (1956) Hydrodynamical study on critical tractive force. *Trans JSCE* 41:1–21
- Jain RK (2008) Influence of cohesion on detachment and transport of clay-sand-gravel mixtures. IIT Roorkee, India
- Kamphuis JW, Hall KR (1983) Cohesive material erosion by unidirectional current. *J Hydraul Eng* 109:49–61
- Kothyari UC, Jain RK (2008) Influence of cohesion on the incipient motion condition of sediment mixtures. *Water Resour Res* 44:1–15
- Kothyari UC, Jain RK (2010) Erosion characteristics of cohesive sediment mixtures. In: *River flow*. pp 815–821
- Kuhnle RA (1993) Incipient motion of sand-gravel sediment mixtures. *J Hydraul Eng* 119:1400–1415
- Mitchener H, Torfs H (1996) Erosion of mud/sand mixtures. *Coast Eng* 29:1–25
- Najafzadeh M, Lim SY (2015) Application of improved neuro-fuzzy GMDH to predict scour depth at sluice gates. *Earth Sci Inf* 8:187–196
- Parker G, Klingeman PC, McLean DG (1982) Bedload and size distribution in paved gravel-bed streams. *J Hydraul Div* 108:544–571
- Patel PL, RangaRaju KG (1996) Fractionwise calculation of bed load transport. *J Hydraul Res* 34:363–379
- Patel PL, RangaRaju KG (1999) Critical tractive stress of nonuniform sediments. *J Hydraul Res* 37:39–58
- Rouse H (1939) An analysis of sediment transportation in the light of fluid turbulence. Technical Report, SCS-TP-25, United State

- Department of Agriculture, Soil Conservation Service, Washington, DC
- Shields IA (1936) Application of similarity principles and turbulence research to bed-load movement (Mitteilungen der PreussischenVersuchsanstalt für Wasserbau und Schiffbau, Berlin). Report No. 167 (W. P. Ott and J. C. van Uchelen, translators), California Institute of Technology, Pasadena, California
- Shroff AV, Shah DL (2003) Soil mechanics and geotechnical engineering, Aa Balkema, ISBN 10: 9058092356
- Singh M, Singh IB, Müller G (2007) Sediment characteristics and transportation dynamics of the Ganga River. *Geomorphology* 86:144–175
- Wu W, Wang SSY, Jia Y (2000) Nonuniform sediment transport in alluvial rivers. *J Hydraul Res* 38:427–434
- Yalin MS (1977) *Mechanics of sediment transportation*, 2nd Edition. Pergamon, New York
- Yalin MS, Karahan E (1979) Inception of sediment transport. *J Hydraul Div ASCE* 105:1433–1443
- Yang CT (1973) Incipient motion and sediment transport. *J Hydraul Div* 99:1679–1704